SIMCor

In-Silico testing and validation of Cardiovascular IMplantable devices

Call: H2020-SC1-DTH-2018-2020 (*Digital transformation in Health and Care*)

Topic: SC1-DTH-06-2020 (*Accelerating the uptake of computer simulations for testing medicines and medical devices*)

Grant agreement No: 101017578

Deliverable 7.1

Definition of model output

Due date of delivery: 30 June 2021

Actual submission date: 30 June 2021

Start of the project: 1 January 2021
End date: 31 December 2023

This project has received funding from the European Union's Horizon 2020 research and innovation programmeunder grant agreement N° 101017578

Reference

Name	SIMCor_D7.1_Definition of model output_TUE_30-06-2021
Lead beneficiary	Technische Universiteit Eindhoven (TUE)
Author(s)	Wouter Huberts (TUE)
Dissemination level	Public
Type	Report
Official delivery date	30 June 2021
Date of validation by the WP Leader	29 June 2021
Date of validation by the Coordinator	**30 June 2021**
Signature of the Coordinator	Titus Kuehne Digital unterschrieben von Titus Kuehne Datum: 2021.06.30 12:41:01 +02'00'

Version log

Issue date	Version	Involved	Comments
24/06/2021	1.0	Wouter Huberts (TUE)	First draft by TUE
28/06/2021	2.0	Jan Brüning (CHA); Claudio Capelle (UCL); Jan Romberg (BIO); Andreas Arndt (BIO)	Internal review by CHA, BIO, UCL
28/06/2021	3.0	Wouter Huberts (TUE)	New version, taking into accounts comments and suggestions
30/06/2021	4.0	Anna Rizzo (LYN)	Final review and formal checking by LYN
30/06/2021	Final	Jan Brüning (CHA)	Submission by PC

Executive summary

The deliverable describes the preliminary definition of the physiological outputs that will be used during virtual patient cohort generation of both heart failure and aortic valve disease patients. We will define clinically measurable outputs that are representative for the patient groups, both before and after, respectively, *transcatheter aortic valve implantation* (TAVI) or insertion of a *pulmonary artery pressure sensor* (PAPS). In addition, clinical targets, related to the clinical performance of the implants, are translated to engineering metrics that can be calculated with physiological models. The targets are paravalvular leakage (TAVI), device migration and vessel perforation (PAPS), and thrombosis (TAVI and PAPS). Finally, we will give output ranges based on literature and simulations that have been conducted prior to the start of the project. These output ranges will be used to remove unrealistic virtual patients (i.e., outside the output ranges) during virtual cohort generation.

Table of contents

List of figures

List of tables

Acronyms

Acronym	Full name
TAVI	TransAortic Valve Implantation
PAPS	Pulmonary Artery Pressure Sensor
HF	Heart failure
PD	Peak dobutamine
SAVI	Stress aortic valve index
WSS	Wall shear stress
OSI	Oscillatory shear index
HO	Hypotensive
N	Normotensive
H-x	Hypertensive, x = MI: mild, M: moderate, S: severe, VS: very severe
AS	Aortic stenosis
PH	Pulmonary hypertension
PAH	Pulmonary arterial hypertension
MPA	Main pulmonary artery
RPA	Right pulmonary artery
LPA	Left pulmonary artery
AAo	Ascending Aorta

Introduction

One of the primary aims of SIMCor is the development and validation of virtual patient cohorts. Ideally, one would like to have a generator that outputs a realistic virtual patient based on features of the true population, i.e., each realisation should have geometrical, demographical, mechanical and physiological features (e.g., blood pressure and wall stresses) that theoretically could exist in the real patient population. Though often enormous amounts of data might be available, it will be almost impossible to obtain the true population distribution due to data sparsity, possible conflicting data between different modalities, the enormous numbers of factors that might span the population space and their mutual dependencies. Moreover, based on data alone, it will be very difficult to create virtual cohorts that have realistic patient features and at the same time mimic the corresponding physiology.

In the past decades, in-silico models of human physiology have been developed and these models can integrate input data into engineering concepts (e.g., pressure, flows, axial forces), thereby relating the data by means of established physiological and physical laws. These models give us the possibility to create virtual patients with meaningful physiological behaviour by varying their input parameters. For example, mass conservation will always be assured in these types of models.

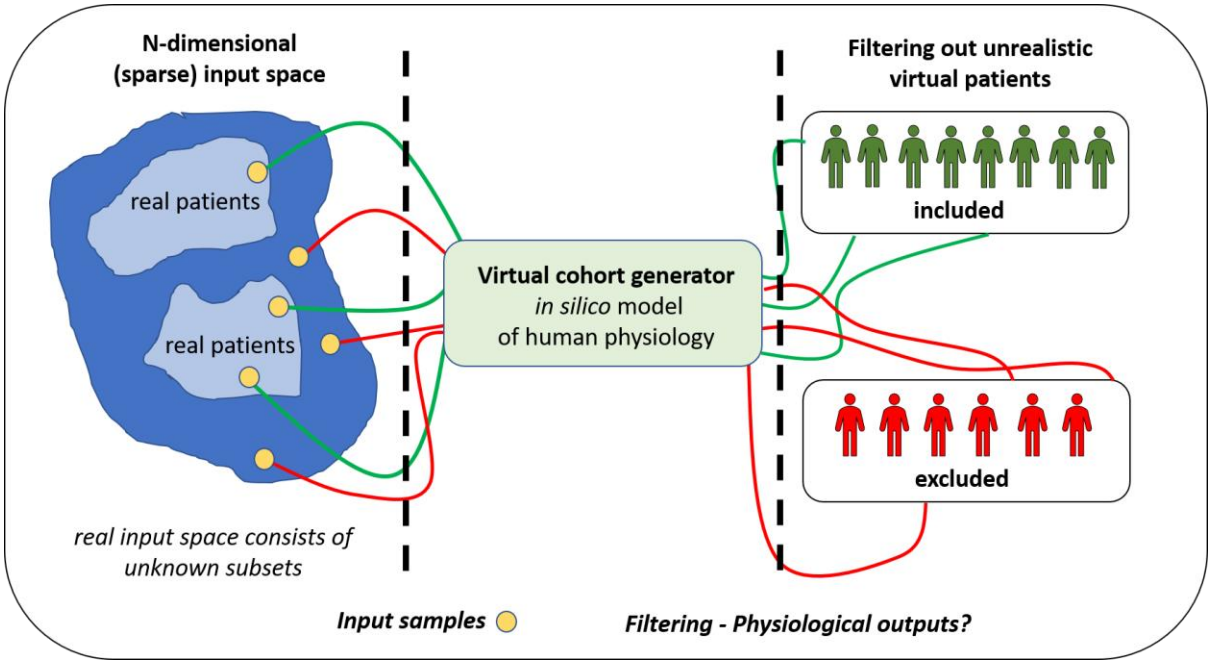

Figure 1: Schematic overview of the SIMCor methodology for virtual cohort generation.

Each model realisation is in fact a possible candidate for our virtual cohort. However, non-physiological candidates might occur due to non-physiological combinations of input parameters caused by the incomplete definition of the true input space. Fortunately, this can be resolved by defining proper model output criteria and their ranges: each candidate that has output of interests outside the predefined ranges can be excluded from our virtual cohorts. These outputs thus serve as criteria to filter out non-physiological virtual patients from our cohort. A schematic overview of the methodology proposed is given in *Figure 1*. Note that this approach assumes that the physiological model used for the creation of virtual patient candidates can accurately simulate the physiology of real patients, which means that model validation has been done on patient-level (i.e., the first level of our three-level validation strategy of the virtual cohorts generated).

In the next subsections, we will describe how we defined the model outputs of interest that are needed for the development of our “filter”. Moreover, we will present the types of sources that we used to define proper population ranges for the output of interests used. A subset of the output ranges will become available during the project, as envisioned in our methodology described in the proposal. Therefore, we will not yet identify correlations between outputs. Moreover, we will not make a full stratification based on demographics, comorbidities, and risk scores as the results of our sensitivity analyses are required to determine the relevant stratification criteria. In the last section, we will explain how we will iteratively improve the definition of the output ranges during the project.

Definition of the outputs of interest

The candidates for the virtual cohort, which are generated by the physiological models, are either added to the cohort or excluded based on output ranges that are representative for the geometry, haemodynamics and physiology of aortic valve stenosis and *heart failure* (HF) patients. Moreover, the physiological response, and the corresponding output ranges, to either *transcatheter aortic valve implantation* (TAVI) or *pulmonary artery pressure sensor* (PAPS) implantation should be realistic. To quantify the latter physiological metrics, we have converted the clinical targets that are related to the clinical performance of the specific devices into engineering metrics that we can calculate with our models, see *Figure 2*. The clinical targets were previously defined as paravalvular leakage (TAVI), device migration and vessel perforation (PAPS), and thrombosis (both TAVI and PAPS).

The definition of the output of interest is based on two important categories, i.e., functional outputs and model-derived outputs that are believed to be important for our clinical targets. Metrics that are required during evaluation of medical devices by regulatory bodies (ISO/DIS 5840-1:2019) are included into the first category. Geometrical data will not be considered in this deliverable but is available (see WP5 and WP6).

Outputs of interest for aortic valve stenosis patients

Functional outputs

First, all virtual patients should have general functional outputs like ventricular and arterial pressures (i.e., mean, systolic and diastolic), transvalvular flow and aortic valve flow velocities (i.e., mean, systolic and diastolic) that are realistically for aortic valve patients. These outputs and their ranges are based on literature[1,2], ISO standards[3] for in-vitro valve testing and/or expert opinions and will serve as the first layer of our "filter". Second, we will complete the outputs and their ranges with functional information that is routinely collected by our partner hospitals before and after TAVI implantation, eventually augmented with simulation data. Details about clinical data collection and statistics can be found in the deliverables of WP5 and WP6.

Echocardiography is considered as the key tool for the diagnosis of aortic valve stenosis as it can confirm the presence of aortic valve stenosis, the degree of valve calcification, left ventricular function and wall thickness. Moreover, it detects other valve disease or aortic pathologies, and it provides useful prognostic information[4]. Doppler echocardiography is currently most often used to quantify the stenosis severity based on pressure gradient estimation using a simplified Bernoulli equation and transvalvular blood flow velocities[2.] Invasive LV catheterization is no longer routinely used to assess the pressure gradient. Its use is restricted to cases where non-invasive modalities are inconclusive.

Also, during follow-up evaluations, echography is very useful to evaluate hemodynamic progression, LV function and hypertrophy and the dimensions of the aorta[4]. A significant number of functional measurements, which are performed during these routine echographic examinations in the clinic, are very well suited to assess the validity of our virtual patients. The ranges of relevant functional metrics that are measured, or derived from the data, within the partner hospitals are summarized in *Table 1*

[1] El Faquir et al., Patient-specific computer simulation in TAVR with the self-expanding Evolut R valve. JACC: Cardiovasc Interv. 2020; 13(5): 1803-1812. doi: 10.1016/j.jcin.2020.04.018.

[2] Bosi et al. A validated computational framework to predict outcomes in TAVI. Nature Scientific Reports 2020; 10:9906. doi: 10.1038/s41598-020-66899-6.

[3] https://www.beuth.de/de/norm-entwurf/iso-dis-5840-1/301539264

[4] Baumgartner et al.; ESC Scientific Document Group. 2017 ESC/EACTS Guidelines for the management of valvular heart disease. Eur Heart J. 2017 Sep 21;38(36):2739-2791. doi: 10.1093/eurheartj/ehx391.

of the next section. The outputs of interest are complemented by state-of-the-art output metrics that are not routinely measured but are believed to be relevant for the diagnosis and intervention planning, a.o. the stress aortic valve index recently introduced by Johnson et al.[5] and applied to low gradient-low flow patients by Zelis et al.[6] .

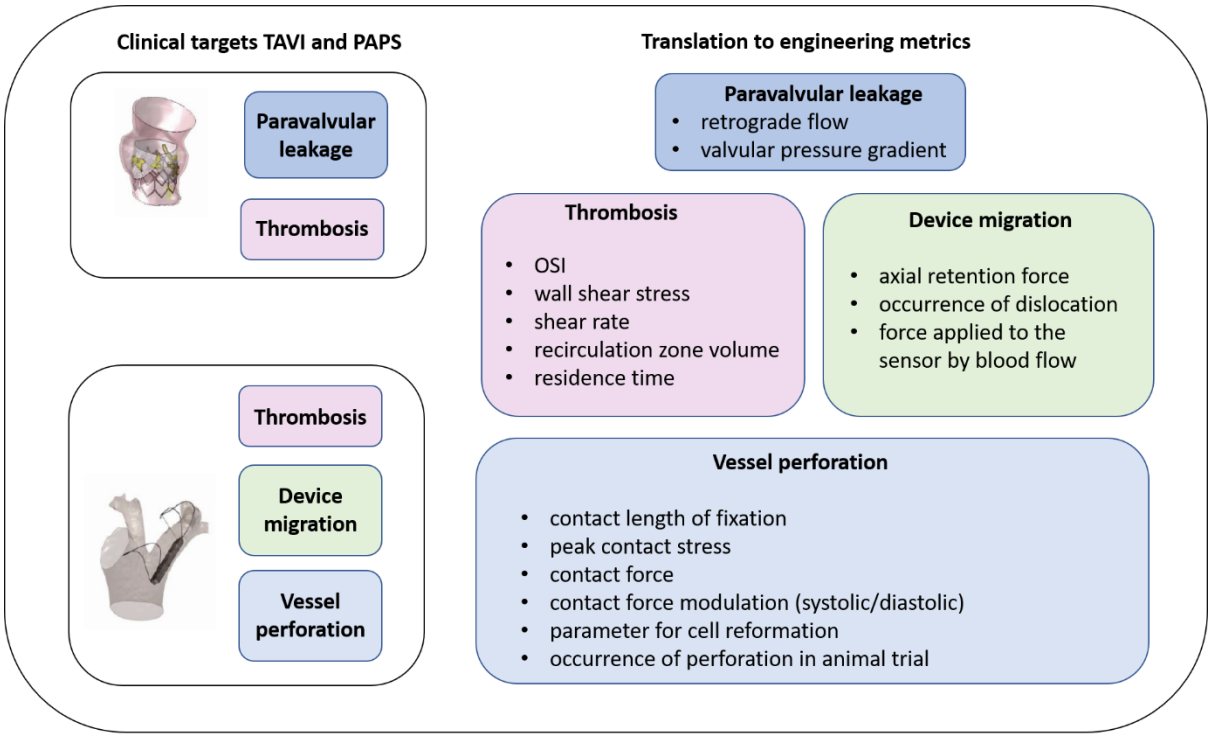

Figure 2: Clinical targets for both the PAPS and TAVI, and the translation of these clinical targets to engineering metrics.

Model-derived metrics related to clinical targets

In addition to the clinical data discussed above, there are also relevant hemodynamic output metrics that are related to our clinical targets and can only be derived by using physics-based mathematical models[7,8,9,10], state-of-the art in-vitro experiments[11,12] and/or imaging modalities for acquisition of 3D velocity fields (e.g. 4D MRI[13]). The hemodynamic factors (see *Figure 2*) that are predictive for thrombus

[5] Johnson et al. Pressure gradient vs. flow relationships to characterize the physiology of a severely stenotic aortic valve before and after transcatheter valve implantation, Eur Heart J. 2018 39:2646-2655, doi: 10.1093/eurheartj/ehy126.

[6] Zelis et al. Stress aortic valve index (SAVI) with dobutamine for low-gradient aortic stenosis: a pilot study. Structural Heart 2020 4(1):53-61. doi: 10.1080/24748706.2019.1690180

[7] Luraghi et al. On the modeling of patient-specific transcatheter aortic valve replacement: a fluid-structure interaction approach. Cardiovasc. Eng. Technol. 2019; 10(3): 437-455. doi: 10.1007/s13239-019-00427-0.

[8] Ghosh et al. Numerical evaluation of transcather aortic valve performance during heart beating and its post-deployment fluid-structure interaction analysis. Biomech Modeling in MechanoBiol. 2020; 19: 1725-1740. doi: 10.1007/s10237-020-01304-9.

[9] Hoeijmakers et al. Estimation of valvular resistance of segmented aortic valves using computational fluid dynamics. J Biomech. 2019; 94: 49-58. doi: 10.1016/j.jbiomech2019.07.010.

[10] Youssefi et al. Patient-specific computational fluid dynamics - assessment of aortic hemodynamics in a spectrum of aortic valve pathologies. J Thorac Cardiovasc Surg. 2017; 153: 8-20. doi: 10.1016/j.jtcvs.2016.09.040.

[11] Yap et al. Experimental measurement of dynamic fluid shear stress on the aortic surface of the aortic valve leaflet. Biomech Model Mechanobiol. 2012; 11: 171-182. doi: 10.1007/s10237-011-0301-7.

[12] Hatoum et al. Impact of patient-specific morphologies on sinus flow stasis in transcatheter aortic valve replacement: an in vitro study. J Thorac Cardiovasc Surg. 2019; 157: 540-9. doi: 10.1016/j.jtcvs.2018.05.086.

[13] Farag et al. Transcatheter aortic valve replacement alters ascending aorta blood flow and wall shear stress patterns: A 4D flow MRI comparison with age-matched, elderly controls. Eur Radiol. 2019; 29: 1444-1451. doi: 10.1007/s00330-018-5672-z.

formation are based on both discussions of our multidisciplinary team, and on relevant studies in literature.

Thrombosis is a major problem for the implantation of aortic valves and patients receiving mechanical artificial valves will get lifelong anticoagulation therapy[14]. It has recently been shown that patients that receive a transcatheter aortic valve replacement commonly develop leaflet thrombosis[15]. Virchow's triad describes the three factors that can lead to thrombosis: circulatory stasis, endothelial cell injury and hypercoagulability. The first two factors are mainly responsible for thrombosis after TAVI. Circulatory stasis describes the abnormalities in haemodynamics, such as disturbed flow created by bifurcations, stenotic regions, and close to the leaflets. Also flow separation and reattachment, low oscillatory wall shear stresses and high residence times are known for increased risk of thrombosis. Several studies have set the risk of platelet activation by defining wall shear stress thresholds and the corresponding exposure time that mark the onset of platelet activation. Hung et al.[16,17] have set WSS thresholds of 10-16.5 Pa with an exposure time of 100 s, while Williams[17,18]. defined a WSS threshold of 13 Pa with an exposure time of 1 millisecond. In another study they used a WSS of 30-100 Pa with an exposure time of 10 milliseconds to 10 seconds, as threshold for platelet activation.[17,19] . The important role of the local haemodynamics makes it evident that we defined haemodynamics metrics to estimate the probability of thrombus formation after TAVI, and to validate whether our virtual patients have a physiological response after AV implantation (see *Figure 2*). The ranges of these output metrics are based on retrospective simulation studies or 4D MR flow measurements, either done by our consortium or other engineering groups that reported their results in scientific journals. In *Table 2* of the next section a complete overview of all relevant simulation outputs and their ranges are listed.

Outputs of interest for heart failure patients in a non-acute setting

Pulmonary hypertension (PH) is a frequent condition, which may occur because of pulmonary vascular disease, chronic left heart or lung disease, pulmonary embolism, or other aetiologies[20] . Regardless of the origin, pulmonary hypertension is defined by a mean pulmonary arterial pressure larger than 25 mmHg. Left heart disease accounts for about 65-80% of all PH cases and is associated with worse clinical outcomes when compared to HF patients without hypertension[21]. Recent randomized clinical trials have demonstrated that adequate monitoring of pulmonary hypertension by means of PAPS significantly reduces hospitalisation for HF patients, irrespectively of ejection fraction[22].

Functional outputs

The functional outputs that we define for the virtual cohort generator of heart failure patients, receiving a PAPS device, are related to pulmonary artery haemodynamics. In addition, we consider metrics that are clinically used to diagnose and monitor pulmonary hypertension associated with heart

[14] Roudaut R et al. Thrombosis of prosthetic heart valves: diagnosis and therapeutic considerations. Heart. 2007;93(1):137-142. doi:10.1136/hrt.2005.071183

[15] Raghav et al. Three-dimensional extent of flow stagnation in transcatheter heart valves. J.R. Soc. Interface 2019 16: 20190063. doi: 10.1098/rsif.2019.0063

[16] Hung et al. Shear-induced aggregation and lysis of platelets. Trans Am Soc Artif Intern Organs 1976;22:285–91

[17] Khodaee et al. Incomplete expansion of transcatheter aortic valves is associated with propensity for valve thrombosis. Interact Cardiovasc Thorac Surg 2020 30: 39-46. doi: 10.1093/icvts/ivz213

[18] Williams AR. Release of serotonin from human platelets by acoustic microstreaming. J Acoust Soc Am 1974;56:1640–9.

[19] Ramstack JM et al. Shear-induced activation of platelets. J Biomech 1979;12:113–25.

[20] Ponikowski et al.; ESC Scientific Document Group. 2016 ESC Guidelines for the diagnosis and treatment of acute and chronic heart failure. Eur Heart J. 2016 37:2129-2200. doi: 10.1093/eurheartj/ehw128..

[21] Rosenkranz et al. Left ventricular heart failure and pulmonary hypertension. Eur Heart J. 2016 37: 942-954. doi: 10.1093/eurheartj/ehv512.

[22] Abraham et al. Wireless pulmonary artery haemodynamic monitoring in chronic heart failure: a randomised controlled trial. Lancet 2011; 377:658-66. doi: 10.1016/s0140-6736(11)60101-3

failure[23,24]. Since it might be challenging to discriminate between pulmonary hypertension due to left heart failure (i.e., postcapillary PH) and pulmonary arterial hypertension (i.e., precapillary PH), we will focus on metrics that are clinically used to make this distinction. Moreover, we will include data of pulmonary haemodynamics in apparently healthy volunteers of different age groups[25]. Most of the data was previously reported in literature and based on clinical modalities such as MRI, ultrasound, or invasive right heart catheterization measurements. In *Table 3* of the next section a complete overview of all relevant simulation outputs and their ranges are listed.

Model-derived metrics related to clinical targets

Also, for the PAPS we have defined engineering metrics that can be calculated by our models. For the clinical target of thrombosis, we are again defining wall shear stress related outputs, and their ranges, based on simulations reported in literature[26] or done by CHA, specifically for this deliverable. This WSS data is complemented by MRI studies[27]. The engineering metrics associated with device migration and perforation logically only consider the situation after PAPS implantation. These engineering metrics are based on preliminary simulations of BIO again specifically conducted for this deliverable. The metrics and their ranges are grouped and presented in *Table 4* of the next section.

[23] Sanz et al. Evaluation of pulmonary artery stiffness in pulmonary hypertension with cardiac magnetic resonance. JACC: Cardiovasc Imaging. 2009; 2(3): 286-95. doi: 10.1016/j.jcmg.2008.08.007.

[24] Heywood et al. Impact of practice-based management of pulmonary artery pressures in 2000 patients implanted with the CardioMEMS sensor. Circulation 2017; 135: 1509-1517. doi: 10.1161/CIRCULATIONAHA.116.026184.

[25] Wehrum et al. Age dependence of pulmonary artery blood flow measured by 4D flow cardiovascular magnetic resonance: results of a population-based study. J Cardiovasc Magnetic Resonance. 2016; 18: 31. doi: 10.1186/s12968-016-0252-3.

[26] Tang et al. Wall shear stress is decreased in the pulmonary arteries of patients with pulmonary hypertension: An image-based computational fluid dynamics study. Pulm Circ 2012; 2: 470-6. doi: 10.4103/2045-8932.105035.s40064-016-2755-7.

[27] Odagiri et al. Non-invasive evaluation of pulmonary arterial blood flow and wall shear stress in pulmonary arterial hypertension with 3D phase contrast magnetic resonance imaging. SpringerPlus 2016; 5: 1071. doi: 10.118

Definition of the output ranges

In this section we will provide a complete overview of all outputs of interest and their ranges. The tables are grouped by clinical application, and we give one table for clinical data and one table in which metrics are given that can only be assessed accurately by means of mathematical modelling, state-of-the art imaging modalities and/or in-vitro experiments. In addition, information regarding the source that is used to define the output ranges is provided in the last column of each table.

Output ranges for aortic valve stenosis patients

Outputs of interest	PRE-TAVI	POST-TAVI	References/sources
Aortic valve regurgitation	*UCL dataset*[a] None-trivial: 29.6% Mild-moderate: 69.2% Moderate-severe:7.8% Severe: 0%	Degree of regurgitation <= moderate (35% regurgitant fraction)[a] Paravalvular leakage circumferential extent (PARS-SAX-SE-score): 8 (13-14)%[b] *Aortic Regurgitation* fraction: 23 (6-27)[b] % volume: 12 (3-21)[b] ml	[a]*Echo data UCL* [b]*El Faquir et al., JACC: Cardiovascular interventions (2020) 13(15):1803-12*
Forward flow volume	*In vitro ISO norms* 25 to 100[c] ml	Not available: TBD	[c]*ISO standards: ISO/DIS 5840-1:2019*
Peak aortic jet velocity	Baseline: 4.1 ± 0.7[a] m/s Baseline: 4.0 ± 0.6[b] m/s	Baseline: 1.94 ± 0.35[c] m/s 1.8±0.4[b] m/s *Device expansion*[d] 100%: 1.40 m/s 90%: 1.51 m/s 80%: 1.79 m/s	[a]*Echo data UCL* [b]*El Faquir et al., JACC: Cardiovascular interventions (2020) 13(15):1803-12* [c]*Echo data CHA* [d]*Khodaee et al., Interactive Cardiovasc Thorac Surg (2020) 30:39-46*
Peak pressure difference (open valve)	*Low gradient stenosis* Baseline: 25 (17-32)[e] mmHg PD: 34 (25-47)[e] mmHg *Severe aortic stenosis* Baseline: 45 (40-53)[f] PD: 67 (53-80)[f] mmHg Baseline: 72 ± 22[a] mmHg Baseline: 64 (55-77)[b] mmHg Baseline: 73 ± 16[g] mmHg	*Severe aortic stenosis* Baseline: 9 (5-11) [f] PD: 13 (8-23) [f] Baseline: 18 ± 7[a]	[a]*Echo data UCL* [b]*El Faquir et al., JACC: Cardiovascular interventions (2020) 13(15):1803-12* [e]*Zelis et al., Structural Heart (2020) 4(1): 53-61* [f]*Johnson et al., European Heart J (2018) 39: 2646-2655* [g]*Bosi et al., Nature Scientific Reports (2020) 10:9906*

Peak pressure difference (closed valve)	*Mock loop settings*[h] HO: <80 mmHg N: 80-115 mmHg H-Mi:115-129 mmHg H-M: 130-144 mmHg H-S: 145-164 mmHg H-VS: > 165 mmHg		[h]*ISO standards: ISO/DIS 5840-1:2019*
Mean pressure difference (open valve)	Baseline: 43 ± 15[c] mmHg Baseline: 41 ± 13[b] mmHg	Baseline: 9 ± 4[c] mmHg Baseline: *7*±3[b] mmHg	[b]*El Faquir et al., JACC: Cardiovascular interventions (2020) 13(15):1803-12* [c]*Echo data UCL*
Arterial peak systolic pressure	*Mock loop settings*[h] N: 90 to 140 mmHg HO: <90 mmHg H-Mi: 140-159 mmHg H-M: 160-179 mmHg H-S: 180-209 mmHg H-VS: > 210 mmHg *Clinical measurements*[b] 144±21 mmHg	Remains almost similar	[b]*El Faquir et al., JACC: Cardiovascular interventions (2020) 13(15):1803-12* [c]*Echo data UCL* [h]*ISO norms: ISO/DIS 5840-1:2019*
Arterial end diastolic pressure	*Mock loop settings*[h] N: 60 to 90 mmHg HO: <60 mmHg H-M:90-99 mmHg H-M: 100-109 mmHg H-S: 110-119 mmHg H-VS: > 120 mmHg *Clinical measurements*[b] *74*±13 mmHg	Remains almost similar	[b]*El Faquir et al., JACC: Cardiovascular interventions (2020) 13(15):1803-12* [c]*Echo data UCL*
Velocity Time Integral (VTI)	*97*±23[b] cm	*32*±7[b] cm	[b]*El Faquir et al., JACC: Cardiovascular interventions (2020) 13(15):1803-12*
LV EF	55 (44-59) [a] *%* 59 (50-65) [b] *%*	58 ± 15[c] % 51 ± 10[b] *%*	[a]*Echo data UCL* [b]*El Faquir et al., JACC: Cardiovascular interventions, 13(15):1803-12 (2020)* [c]*Echo data CHA*
LV SV	68.7± 21[a] ml	79.1 ± 24.9[c] ml	[a]*Echo data UCL*

			[c]*Echo data CHA*
SAVI [-]	*Low gradient stenosis* Baseline: 0.81 (0.74-0.86) [e] PD: 0.76 (0.68-0.81) [e] *Severe aortic stenosis* Baseline: 0.63 (0.59-0.67) [f] PD: 0.56 (0.48-0.58) [f]	*Severe aortic stenosis* Baseline: 0.90 (0.87-0.93) [f] PD: 0.86 (0.81-0.90) [f]	[e]*Zelis et al., Structural Heart (2020) 4(1): 53-61* [f]*Johnson et al., European Heart J (2018) 39: 2646-2655*
Heart rate	*Low gradient stenosis* Baseline: 75 ± 15[e] bpm PD: 103 ± 22[e] bpm *Severe aortic stenosis* Baseline: 62 ± 14[f] bpm PD: 94 ± 21[f] bpm *Mock loop settings*[h] 30 to 200 bpm	*Severe aortic stenosis* Baseline: 68 ± 12[f] bpm PD: 88 ± 23[f] bpm	[e]*Zelis et al., Structural Heart (2020) 4(1): 53-61* [f]*Johnson et al., European Heart J (2018) 39: 2646-2655* [h]*ISO standards s: ISO/DIS 5840-1:2019*
Left ventricular systolic pressure	*Low gradient stenosis* Baseline: 133 ± 17[e] mmHg PD: 144 ± 29[e] mmHg *Severe aortic stenosis* Baseline: 130 ± 23[f] mmHg PD: 158 ± 26[f] mmHg	*Severe aortic stenosis* Baseline: 101 ± 25[e] mmHg PD: 125 ± 33[f] mmHg	[e]*Zelis et al., Structural Heart (2020) 4(1): 53-61* [f]*Johnson et al., European Heart J (2018) 39: 2646-2655*
Aortic systolic pressure	*Low gradient stenosis* Baseline: 107 ± 14[e] mmHg PD: 107 ± 26[e] mmHg *Severe aortic stenosis* Baseline: 83 ± 15[f] mmHg PD: 89 ± 24[f] mmHg	*Severe aortic stenosis* Baseline: 92 ± 26[f] mmHg PD: 109 ± 35[f] mmHg	[e]*Zelis et al., Structural Heart (2020) 4(1): 53-61* [f]*Johnson et al., European Heart J (2018) 39: 2646-2655*
Systolic portion of	*Low gradient*		[e]*Zelis et al., Structural Heart (2020)*

cardiac cycle	*stenosis* Baseline: 34 ± 4[e] % PD: 35 ± 6[e]% *Severe aortic stenosis* Baseline: 33 ± 4[f]% PD: 37 ± 5[f] %	*Severe aortic stenosis* Baseline: 30 ± 7[f] % PD: 29 ± 7[f] %	*4(1): 53-61* *[f]Johnson et al., European Heart J (2018) 39: 2646-2655*
Cardiac output	*Low gradient stenosis* Baseline: 5.4 ± 1.0[e] l/min PD: 7.6 ± 0.6[e] l/min *Severe aortic stenosis* Baseline: 3.2 ± 0.6[f] l/min PD: 6.0 ± 2.2[f] l/min *Mock loop settings[h]* 3 to 15 l/min	*Severe aortic stenosis* Baseline: 3.6 ± 1.0[f] l/min PD: 5.9 ± 1.9[f] l/min	*[e]Zelis et al., Structural Heart (2020) 4(1): 53-61* *[f]Johnson et al., European Heart J (2018) 39: 2646-2655* *[h]ISO standard s: ISO/DIS 5840-1:2019*
Transvalvular systolic flow	*Low gradient stenosis* Baseline: 268 (240-291)[e] ml/s PD: 380 (354-424)[e] ml/s *Severe aortic stenosis* Baseline: 162 (143-186)[f] ml/s PD: 270 (198-311)[f] ml/s	*Severe aortic stenosis* Baseline: 224 (163-290)[f] ml/s PD: 340 (282-445)[f] ml/s	*[e]Zelis et al., Structural Heart (2020) 4(1): 53-61* *[f]Johnson et al., European Heart J (2018) 39: 2646-2655*
Stroke Volume index	*Low gradient stenosis* Baseline: 37 ± 11[e] ml/m^2 PD: 46 ± 12[e] ml/m^2 *Severe aortic stenosis* Baseline: 29 ± 7[f] ml/m^2 PD: 34 ± 11[f] ml/m^2	Severe aortic stenosis Baseline: 29 ± 11[b] ml/m^2 PD: 36 ± 11[b] ml/m^2	*[e]Zelis et al., Structural Heart (2020) 4(1): 53-61* *[f]Johnson et al., European Heart J (2018) 39: 2646-2655*

Table 1: Ranges of the outputs of interest for aortic valve stenosis patients based on clinical data, before and after TAVI. The ranges are either given as mean ± standard deviation or as median (interquartile range).

Outputs of interest	PRE-TAVI	POST-TAVI	References/sources
Aortic valve regurgitation volume [ml]	Not yet available: TBD	Mild: 26.88[a] ml Moderate: 43.73[a] ml *Valve positioning*[b] Midway: 41.61 ml Ventricular: 34.59 ml	[a]*Luraghi et al., Cardiovasc Eng and Technol (2019) 10(3): 437–455* [b]*Ghosh et al., Biomech Modeling Mechanobiol (2020) 19:1725–1740*
Closing volume	Not yet available: TBD	*Valve positioning*[b] Midway: 14.28 ml Ventricular: 6.87 ml	[b]*Ghosh et al., Biomech Modeling Mechanobiol (2020) 19:1725–1740*
Maximum velocity in vena contracta range	0.88-5.36[c] m/s	1-1.4[d] m/s	[c]*Hoeijmakers et al., Journal of Biomechanics 94 (2019) 49–58* [d]*Kodhaee et al, Interactive Cardiovasc Thorac Surg (2019) 30: 39-46*
Effective pressure difference	2.5-102.5[c] mmHg	Back to non-pathological situation	[c]*Hoeijmakers et al., Journal of Biomechanics 94 (2019) 49–58*
Simplified Bernouilli pressure difference	3.1-115.1[c] mmHg	Back to non-pathological situation	[c]*Hoeijmakers et al., Journal of Biomechanics 94 (2019) 49–58*
Residence time	Not yet available; TBD	*Percentage on leaflet >0.5 s for different levels of valve expansion*[d] 100%: 70.4% 90%: 84.4% 80%: 93.4% Range: 0.2 to 0.8[d] s	[d]*Kodhaee et al, Interactive Cardiovasc Thorac Surg (2019) 30: 39-46*
Relative residence time	Not yet available; TBD	Not yet available; TBD	
Shear rate	Not yet available; TBD	Not yet available; TBD	
Mean Wall shear stress	*Ascending aorta*[e] Controls: 0.98±0.54 Pa AS-Tricuspid: 3.50±2.01 Pa AS-Bicuspid (R-L cusp fusion): 2.73±1.00 Pa AS-Bicuspid (R-no cusp fusion): 3.71±0.40 Pa	*On the aortic wall*[f] TAVR: 0.36 ± 0.54 Pa C: 0.24 ± 0.09 Pa	[e]*Youssefi et al., J Thorac Cardiovasc Surg (2017) 153:8-20* [f]*Farag et al., European Radiology (2019) 29:1444–1451*
Peak Wall shear stress	*Aortic surface of valve leaflet*[g]	*On the aortic wall*[f] TAVR: 0.90 ± 0.25 Pa Controls: 0.62 ± 0.33 Pa	[d]*Kodhaee et al, Interactive Cardiovasc Thorac Surg (2019) 30: 39-46*

	1.50 Pa±5% HR: 70 bpm SV: 68 ml 1.34 Pa ±6% HR: 70 bpm SV: 62 ml 0.64 Pa ±14% HR: 70 bpm SV: 43 ml 0.11 Pa ±62% HR: 70 bpm SV: 29 ml 1.14 Pa ±25% HR: 50 bpm SV: 55 ml 1.02 Pa ±36% HR: 70 bpm SV: 55 ml 0.78 Pa ±47% HR: 90 bpm SV: 68 ml	*On the valve leaflet[d] (ventricular side)* 0-10 Pa	*[f]Farag et al., European Radiology (2019) 29:1444–1451* *[g]Yap et al., Biomech Model Mechanobiol (2012) 11:171-182*
Diastolic wall shear stress magnitude in the subregion adjacent to the leaflet	Not yet available: TBD	*CoreValve[h]* Aortic root Model 1 (M1): upto 0.25 Pa Aortic root Model 2 (M2): upto 0.5 Pa *SAPIEN[h]* Aortic root M1: upto 0.15 Pa Aortic root M2: upto 0.95 Pa	*[h]Hatoum et al., J Thorac Cardiovasc Surgery (2019) 157(2):540-549*
Systolic wall shear stress magnitude in the subregion adjacent to the leaflet	Not yet available: TBD	*CoreValve[h]* Aortic root M1: upto 0.2 Pa Aortic root M2: upto 0.8 Pa *SAPIEN[h]* Aortic root M1: upto 0.4 Pa Aortic root M2: upto 1.2 Pa	*[h]Hatoum et al., J Thorac Cardiovasc Surgery (2019) 157(2):540-549*
Complete washout of particles remaining in the sinus	Not yet available: TBD	CoreValve[h] Aortic root M1: 3.5 cardiac cycles Aortic root M2: 10 cardiac cycles (still about 18% of the particles remain) *SAPIEN[h]* Aortic root M1: 1.25 cardiac cycles Aortic root M2: 7.5 cardiac cycles	*[h]Hatoum et al., J Thorac Cardiovasc Surgery (2019) 157(2):540-549*
Oscillatory shear index [-]	*Ascending aorta[e]* Controls: 0.18±0.04 AS-Tricuspid: 0.19±0.02 AS-Bicuspid (R-L cusp fusion): 0.18±0.03 AS-Bicuspid (R-no	*Midway valve positioning[b]* On RC leaflet: 0.0074 NC leaflet: 0.1860 LC leaflet: 0.0715 *Ventricular valve positioning[b]* On RC leaflet: 0.0618 NC leaflet: 0.0855	*[b]Ghosh et al., Biomech Modeling Mechanobiol (2020) 19:1725–1740* *[e]Youssefi et al., J Thorac Cardiovasc Surg (2017) 153:8-20*

	cusp fusion): 0.13±0.02	LC leaflet: 0.0337	
Area-weighted WSS	Not yet available: TBD	*Range over leaflet type and valve positioning*[b] 3.6-5.2 Pa	[b]*Ghosh et al., Biomech Modeling Mechanobiol (2020) 19:1725–1740*
Vorticity in sinus region and adjacent the TAV leaflets	Not yet available: TBD	*CoreValve*[h] Aortic root M1: 75 ± 1.1 s^{-1} Aortic root M2: 77± 3.2 s^{-1} *SAPIEN*[h] Aortic root M1: 109 ± 2.3 s^{-1} Aortic root M2: 250± 4.1 s^{-1}	[h]*Hatoum et al., J Thorac Cardiovasc Surgery (2019) 157(2):540-549*
Maximum velocity in sinus region and adjacent the TAV leaflets at peak systole	Not yet available: TBD	*CoreValve*[h] M1: 0.13 ± 0.01 m/s M2: 0.10± 0.02 m/s *SAPIEN*[h] M1: 0.30 ± 0.02 m/s M2: 0.34± 0.041 m/s	[h]*Hatoum et al., J Thorac Cardiovasc Surgery (2019) 157(2):540-549*

Table 2: Ranges of the model-derived outputs of interest for aortic valve stenosis patients before and after TAVI. The ranges are either given as mean ± standard deviation or as median (interquartile range).

Output ranges for heart failure patients in a non-acute setting

Outputs of interest	PRE-PAPS	POST-PAPS	References/sources
Systolic pulmonary artery pressure	PAH[b]: 88±14 mmHg *No PH*[c] 24 (22–29) mmHg *Exercise-induced PH*[c] 32 (24–36) mmHg *PH at rest*[c] 70 (60–82) mmHg	*CHAMPION cohort*[a] Baseline, Control (C)+Treatment (T) group: 46.4±14.5 mmHg *Real World cohort*[a] Baseline (B): 49.7±14.1 mmHg	[a]*Heywood et al., Circulation (2017) 135:1509-1517* [b]*Tang et al., Pulm Circ (2012) 2(4): 470-476* [c]*Sanz et al., JACC: Cardiovasc Imag (2009) 2(3): 286-295*
Mean pulmonary artery pressure	*PAH[b]:* 57±9 mmHg *No PH*[c] 15 (14–18) mmHg *Exercise-induced PH*[c] 15 (14–18) mmHg *PH at rest*[c] 43 (35–40) mmHg	*CHAMPION cohort*[a] Baseline, C+T: 31.6±10.7 *Real World cohort*[a] Baseline: 34.9±10.2	[a]*Heywood et al., Circulation (2017) 135:1509-1517* [b]*Tang et al., Pulm Circ (2012) 2(4): 470-476* [c]*Sanz et al., JACC: Cardiovasc Imag (2009) 2(3): 286-295*
Diastolic pulmonary artery pressure	*PAH[b]:* 38±5 *No PH*[c] 9 (8–12) mmHg *Exercise-induced PH*[c] 9 (7–11) mmHg *PH at rest*[c] 28 (20–35) mmHg	*CHAMPION cohort*[a] Baseline, C+T: 24.5±9.1 mmHg *Real World cohort*[a] Baseline: 25.4±8.3 mmHg	[a]*Heywood et al., Circulation (2017) 135:1509-1517* [b]*Tang et al., Pulm Circ (2012) 2(4): 470-476* [c]*Sanz et al., JACC: Cardiovasc Imag (2009) 2(3): 286-295*
Pulmonary artery wedge pressure	*No PH*[c] 6 (5–9) mmHg *Exercise-induced PH*[c]		[c]*Sanz et al., JACC: Cardiovasc Imag (2009) 2(3): 286-295*

	6 (5–9) mmHg *PH at rest*[c] 10 (7–12) mmHg		
Heart rate	*Different ages groups of healthy controls*[d] 20-39y: 67.16±7.9 bpm 40-59yr: 65.55±7.7 bpm 60-80yr: 66.1±9.1 bpm	*CHAMPION cohort*[e] Baseline C: 73±12 bpm T: 72±13 bpm	[d]*Wehrum et al., Journal of Cardiovasc Magn Reson (2016) 18:31* [e]*Abraham et al., The Lancet (2011) 377: 658-666*
Pulmonary vascular resistance (PVR)	*PAH*[b]*:* 22.1±9.7 Wood units *PVR index*[c] *No PH* 2.7 (1.8–4.4) Wood unit m^2 *Exercise-induced PH* 2.5 (2.2–3.5) Wood unit m^2 *PH at Rest* 10.6 (6.7–17) Wood unit m^2	Likely to be unchanged	[b]*Tang et al., Pulm Circ (2012) 2(4): 470-476* [c]*Sanz et al., JACC: Cardiovasc Imag (2009) 2(3): 286-295*
Pulsatility – relative change in cross-sectional area during the cardiac cycle	*No PH*[c] 55.2 (27.3–64.6) *%* *Exercise-induced PH*[c] 38.8 (27.4-49) *%* *PH at Rest*[c] 17.2 (14.1-22.7) *%*	Likely to be unchanged	[c]*Sanz et al., JACC: Cardiovasc Imag (2009) 2(3): 286-295*
Distensibility-relative change in cross-sectional area per change of pressure	*No PH*[c] 3.1 (2-4.3) *%/mmHg* *Exercise-induced PH*[c] 1.9 (1.2-2.6) *%/mmHg* *PH at Rest*[c]	Likely to be unchanged	[c]*Sanz et al., JACC: Cardiovasc Imag (2009) 2(3): 286-295*

	0.4 (0.3-2.6) *%/mmHg*		
LV EF	*Different age groups of healthy controls*[d] *20-39y:* 56.6±20.7 % *40-59yr:* 57.6±19.2 % *60-80yr:* 53.6±22.5 %	*CHAMPION cohort*[a] *Baseline EF>40%:* 21.72% of all cases *Real World cohort*[a] *EF >40%* Baseline: 33.79% of all cases *Mean EF : 33.5%, range 5-75%*	[a]*Heywood et al., Circulation (2017) 135:1509-1517* [d]*Wehrum et al., Journal of Cardiovasc Magn Reson (2016) 18:31*
RV EF	*Healthy controls*[f]*:* 45.8±6.7 % *PAH*[f]*:* 43.5±16.0 %	Likely to be unchanged	[f]*Odagiri et al., SpringerPlus (2016) 5:1071*
Time-to-peak values in % of the cardiac cycle for peak antegrade systolic flow .	*Different age groups of healthy controls*[d] *20-39yr* MPA: 17.25±3.58 % LPA: 17.32±6.29 % RPA: 18.23±3.52 % AAo: 15.06±4.59 % *40-59yr* MPA: 15.31±3.02 % LPA: 14.65±2.46 % RPA: 16.24±2.62 % AAo: 14.89±5.48 % *60-80yr* *MPA:* *15.38±3.20 %* LPA: 15.47±2.50 % RPA: 16.56±7.92 % AAo: 13.46±2.70 %	Likely to be unchanged	[d]*Wehrum et al., Journal of Cardiovasc Magn Reson (2016) 18:31*

Time-to-peak values in % of the cardiac cycle for early diastolic retrograde flow	*Different age groups of healthy controls*[d] *20-39yr* *MPA: 43.52±7.45 %* *LPA: 45.26±8.30 %* *RPA: 46.69±10.01 %* *AAo: 41.18±9.614 %* *40-59yr* *MPA: 43.16±5.91 %* *LPA: 44.52±8.29 %* *RPA: 49.02±13.89 %* *AAo: 39.51±6.17 %* *60-80yr* *MPA: 43.53±4.63 %* *LPA: 50.97±13.58 %* *RPA: 49.97±13.65 %* *AAo: 40.6±4.33 %*	Likely to be unchanged	[d]*Wehrum et al., Journal of Cardiovasc Magn Reson (2016) 18:31*
Time-to-peak values in % of the cardiac cycle for diastolic antegrade flow	*Different age groups of healthy controls*[d] *20-39yr* *MPA: 59.85±9.296 %* *LPA:* 61.06 ± 8.991 *%* *RPA:* 61.72 ± 10.15 *%* *AAo:* 55.71 ± 10.03 *%* *40-59yr* *MPA:* 59.37 ± 6.307 *%* *LPA:* 60.99 ± 7.276 *%* *RPA:* 62.63 ± 9.908 *%* *AAo:* 57.76 ± 7.792 *%* *60-80yr*	Likely to be unchanged	[d]*Wehrum et al., Journal of Cardiovasc Magn Reson (2016) 18:31*

	MPA: 60.53 ± 8.112 *%* *LPA:* 66.76 ± 10.14 *%* *RPA:* 63.11 ± 10.83 *%* *AAo:* 61.96 ± 9.991 *%*		
Peak velocity	*Healthy controls[f,*]* MPA: 0.41±0.10 m/s RPA: 0.41±0.15 m/s LPA: 0.32±0.10 m/s *PAH[f]* MPA: 0.28±0.09 m/s RPA: 0.22±0.07 m/s LPA: 0.18±0.07 m/s *Different age groups of healthy controls[d]* *20-39yr* *MPA:* 0.88 ± 0.17 m/s *LPA:* 0.85 ± 0.26 m/s *RPA:* 0.91 ± 0.18 m/s *AAo:* 0.71 ± 0.16 m/s *40-59yr* *MPA:* 0.88 ± 0.16 m/s *LPA:* 0.70 ± 0.16 m/s *RPA:* 0.79 ± 0.15 m/s *AAo:* 0.58 ± 0.15 m/s *60-80yr* *MPA:* 0.95 ± 0.29 m/s *LPA:* 0.65 ± 0.23 m/s *RPA:* 0.78 ± 0.23 m/s	Likely to be unchanged	*[d]Wehrum et al., Journal of Cardiovasc Magn Reson (2016) 18:31* *[f]Odagiri et al., SpringerPlus (2016) 5:1071* **These values seem to be rather low when considering a normal cardiac output and valve opening area. Note that also only five volunteers were included and that the reported cardiac output was indeed only 3.14 l/min.*

	AAo: 0.46 ± 0.14 m/s		
Mean velocity	*Healthy controls[f,*]* MPA: 0.10±0.02 m/s RPA: 0.11±0.04 m/s LPA: 0.09±0.02 m/s *PAH[f]* MPA: 0.07±0.02 m/s RPA: 0.06±0.02 m/s LPA: 0.06±0.05 m/s *Different age groups of healthy controls[d]* *20-39yr* MPA: 0.23 ± 0.04 m/s LPA: 0.23 ± 0.05 m/s RPA: 0.25 ± 0.05 m/s AAo: 0.25 ± 0.05 m/s *40-59yr* MPA: 0.23 ± 0.04 LPA: 0.19 ± 0.03 RPA: 0.23 ± 0.03 AAo: 0.23 ± 0.04 *60-80yr* MPA: 0.23 ± 0.07 *LPA:* 0.18 ± 0.05 *RPA:* 0.21 ± 0.05 *AAo:* 0.21 ± 0.05	Likely to be unchanged	*[d]Wehrum et al., Journal of Cardiovasc Magn Reson (2016) 18:31* *[f]Odagiri et al., SpringerPlus (2016) 5:1071* **These values seem to be rather low again.*
Peak systolic antegrade flow rate	*Healthy controls[f]* MPA: 13.54±2.83 l/min RPA: 5.87±1.08 l/min LPA: 5.10±1.50 l/min	Likely to be unchanged	*[d]Wehrum et al., Journal of Cardiovasc Magn Reson (2016) 18:31* *[f]Odagiri et al., SpringerPlus (2016) 5:1071*

	PAH[f] MPA: 12.74±3.49 l/min RPA: 5.96±1.05 l/min LPA: 4.85±2.83 l/min *Different age groups of healthy controls*[d] *20-39yr* MPA: 354.2 ± 98.7 ml/s LPA: 170.4 ± 50.3 ml/s RPA: 186.4 ± 48.5 ml/s AAo: 398.5 ± 128.6 ml/s *40-59yr* MPA: 344.3 ± 92.6 ml/s LPA: 150.4 ± 45.6 ml/s RPA: 173.4 ± 44.6 ml/s AAo: 343.1 ± 113.6 ml/s *60-80yr* MPA: 328.8 ± 93.2 ml/s LPA: 133.5 ± 56.9 ml/s RPA: 157.3 ± 41.2 ml/s AAo: 327.1 ± 85.2 ml/s		
Peak diastolic antegrade flow rate	*Different age groups of healthy controls*[d] *20-39yr* MPA: 52.1 ± 18.53 ml/s LPA: 35.0 ± 11.83 ml/s RPA: 28.1 ± 10.78 ml/s AAo: 33.9 ± 14.46 ml/s	Likely to be unchanged	[d]*Wehrum et al., Journal of Cardiovasc Magn Reson (2016) 18:31*

	40-59yr MPA: 38.6 ± 15.62 ml/s LPA: 22.2 ± 9.04 ml/s RPA: 20.5 ± 9.71 ml/s AAo: 29.5 ± 10.74 ml/s *60-80yr* MPA: 29.4 ± 11.17 ml/s LPA: 13.4 ± 8.5 ml/s RPA: 17.1 ± 8.83 ml/s AAo: 18.6 ± 8.07 ml/s		
Stroke volume per cardiac cycle	*Different age groups of healthy controls*[d] *20-39yr* MPA: 79.72 ± 19.41 ml/cycle LPA: 39.01 ± 8.11 ml/cycle RPA: 43.07 ± 11.05 ml/cycle AAo: 82.21 ± 20.96 ml/cycle *40-59yr* MPA: 74.89 ± 17.12 ml/cycle LPA: 33.35 ± 7.76 ml/cycle RPA: 39.86 ± 8.68 ml/cycle AAo: 73.39 ± 15.64 ml/cycle *60-80yr* MPA: 71.65 ± 13.87 ml/cycle LPA: 29.58 ± 8.04 ml/cycle RPA: 37.04 ± 8.06 ml/cycle AAo: 66.48 ± 13.93 ml/cycle *Healthy controlsf* *MPA: 62.5±15.6*	Likely to be unchanged	[d]*Wehrum et al., Journal of Cardiovasc Magn Reson (2016) 18:31* [f]*Odagiri et al., SpringerPlus (2016) 5:1071*

	ml *RPA: 30.5±5.8 ml* *LPA: 27.4±7.5 ml* *PAHf* *MPA: 54.9±7.3* *RPA: 32.7±10.6* *LPA: 27.7±12.0*		
Fraction of the retrograde flow	*Different age groups of healthy controls*[d] *20-39yr* MPA: 3.41 ± 2.74 % LPA: 2.58 ± 1.65 % RPA: 1.49 ± 1.20 % AAo: 1.20 ± 1.12 % *40-59yr* MPA: 2.09 ± 1.29 % LPA: 1.48 ± 1.28 % RPA: 0.95 ± 0.79 % AAo: 1.34 ± 1.05 % *60-80yr* MPA: 2.43 ± 1.76 % LPA: 2.03 ± 2.13 % RPA: 1.66 ± 1.42 % AAo: 2.25 ± 2.77 %	Likely to be unchanged	[d]*Wehrum et al., Journal of Cardiovasc Magn Reson (2016) 18:31*
Cardiac output	*Healthy controls*[f] MPA: 3.14±0.77 l/min RPA: 1.53±0.29 l/min LPA: 1.38±0.38 l/min *PAH*[f] MPA: 2.78±0.34 l/min RPA: 1.65±0.55 l/min LPA: 1.41±0.62 l/min *Different age groups of healthy controls*[d] *20-39y:* AA0: 5.33±1.56	Likely to be unchanged	[b]*Tang et al., Pulm Circ (2012) 2(4): 470-476* [d]*Wehrum et al., Journal of Cardiovasc Magn Reson (2016) 18:31* [f]*Odagiri et al., SpringerPlus (2016) 5:1071*

	l/min *40-59yr:* 4.77±0.99 l/min *60-80yr:* 4.39±1.08 l/min *PAH[b]* MPA: 3.7±1.2 l/min *Healthy controls[b]* MPA: 5.8±0.6 l/min		
Cardiac index	*No PH[c]* 3.6 (2.7–3.8) l/min/m^2 *Exercise-induced PH[c]* 3.3 (2.5–3.6) l/min/m^2 *PH at Rest[c]* 3.2 (2.3–3.7) l/min/m^2	Likely to be unchanged	*[c]Sanz et al., JACC: Cardiovasc Imag (2009) 2(3): 286-295*

Table 3: Table 3: Ranges of the outputs of interest for heart failure patients based on clinical data, before and after PAPS implantation. The ranges are either given as mean ± standard deviation or as median (interquartile range).

Outputs of interest	PRE-PAPS	POST-PAPS	References/sources
OSI	not yet available; TBD	not yet available; TBD	
Mean WSS	*Healthy controls[b]* MPA: 0.47±0.07 Pa RPA: 0.59±0.13 Pa LPA: 0.56±0.08 Pa *PAH[b]* MPA: 0.46±0.09 Pa RPA: 0.35±0.17 Pa LPA: 0.39±0.07 Pa *TAWSS averaged over proximal and distal strips of the LPA and RPA[c]* *Proximal* PHA: 0.4±0.3 Pa Controls: 2.1±0.4	*On sensor[a]* *Average [Pa]:* 2.5 (Loc . 1, flow 350 ml/s) 0.9(Loc. 2, flow 350 ml/s) 1.0 (Loc. 3, flow 350 ml/s) 1.4 (Loc. 4, flow 350 ml/s) *Average+SD [Pa]:* 4.1 (Loc . 1, flow 450 ml/s) 2.2 (Loc. 2, flow 450 ml/s) 1.7 (Loc. 3, flow 450 ml/s)	*[a]Simulations conducted by dr. Bruning, CHA* *[b]Odagiri et al., SpringerPlus (2016) 5:1071* *[c]Tang et al., Pulm Circ (2012) 2(4): 470-476*

	Pa *Distal* PHA: 1.0±0.1 Pa Controls: 1.4±0.1 Pa	2.2 (Loc. 4, flow 450 ml/s) *Average-SD [Pa]:* 1.1 (Loc . 1, flow 250 ml/s) 0.4 (Loc. 2, flow 250 ml/s) 0.6 (Loc. 3, flow 250 ml/s) 1.0 (Loc. 4, flow 250 ml/s) *On vessel[a]* *Average [Pa]:* 1.8 (Loc . 1, flow 350 ml/s) 1.8 (Loc. 2, flow 350 ml/s) 1.8 (Loc. 3, flow 350 ml/s) 1.8 (Loc. 4, flow 350 ml/s) *Average+SD [Pa]:* 2.7 (Loc . 1, flow 450 ml/s) 2.7 (Loc. 2, flow 450 ml/s) 2.7 (Loc. 3, flow 450 ml/s) 2.7 (Loc. 4, flow 450 ml/s) *Average-SD [Pa]:* 1.1 (Loc . 1, flow 250 ml/s) 1.1 (Loc. 2, flow 250 ml/s) 1.1 (Loc. 3, flow 250 ml/s) 1.1 (Loc. 4, flow 250 ml/s)	
Maximum WSS	*Healthy controls[b]* MPA: 1.43±0.35 Pa RPA: 1.65±0.68 Pa LPA: 1.58±0.50 Pa *PAH[b]* MPA: 0.93±0.23 Pa	*On sensor[a]* *Average [Pa]:* 43.5 (Loc . 1, flow 350 ml/s) 15.2 (Loc. 2, flow 350 ml/s) 7.9 (Loc. 3, flow 350 ml/s)	*[a]Simulations conducted by dr. Bruning, CHA* *[b]Odagiri et al., SpringerPlus (2016) 5:1071*

	RPA: 0.77±0.23 Pa LPA: 0.64±0.22 Pa	14.4 (Loc. 4, flow 350 ml/s) *Average+SD [Pa]:* 59.4 (Loc . 1, flow 450 ml/s) 24.2 (Loc. 2, flow 450 ml/s) 26.3 (Loc. 3, flow 450 ml/s) 24.1 (Loc. 4, flow 450 ml/s) *Average-SD [Pa]:* 23.1 (Loc. 1, flow 250 ml/s) 5.7 (Loc. 2, flow 250 ml/s) 3.9 (Loc. 3, flow 250 ml/s) 8.9 (Loc. 4, flow 250 ml/s) *On vessel[a]* *Average [Pa]:* 108.6 (Loc . 1, flow 350 ml/s) 108.6 (Loc. 2, flow 350 ml/s) 108.6 (Loc. 3, flow 350 ml/s) 108.6 (Loc. 4, flow 350 ml/s) *Average+SD [Pa]:* 142.1 (Loc . 1, flow 450 ml/s) 142.1 (Loc. 2, flow 450 ml/s) 142.1 (Loc. 3, flow 450 ml/s) 142.1 (Loc. 4, flow 450 ml/s) *Average-SD [Pa]:* 76.2 (Loc . 1, flow 250 ml/s) 76.2 (Loc. 2, flow 250 ml/s) 76.2 (Loc. 3, flow 250 ml/s) 76.2 (Loc. 4, flow 250 ml/s)	

Shear rate	not yet available; TBD	not yet available; TBD	
Recirculation zone volume	not yet available; TBD	not yet available; TBD	
Axial retention force	not applicable	min: 0.005 N, typ: 0.020 N, max: 0.05 N	[d]*Information provided by dr. Ingmar Stade (BIO) based on simulations*
Occurrence of dislocation	not applicable	yes/no	
Contact length of fixation	not applicable	min: 25 mm, typ: 42 mm, max: 50 mm[d+e]	[d]*Information provided by dr. Ingmar Stade (BIO) based on simulations* [e]*Annotation: PAPS contains two fixation elements. Therefore, for the whole device the contact force and contact length these values exist twice and in an easy approximation can be calculated by applying a factor of 2. All other parameters are independent of that.*
Peak contact force	not applicable	min: 0.003 N, typ: 0.01 N, max: 0.05 N	[d]*Information provided by dr. Ingmar Stade (BIO) based on simulations*
Contact force	not applicable	min: 0.05 N, typ: 0.15 N, max: 0.5 N	[d]*Information provided by dr. Ingmar Stade (BIO) based on simulations* [e]*Annotation: PAPS contains two fixation elements. Therefore, for the whole device the contact force and contact length these values exist twice and in an easy approximation can be calculated by applying a factor of 2. All other parameters are independent of that.*
Contact force modulation (systolic/diastolic and breath)	not applicable	min: 10 %, typ: 15 %, max: 25 %	[d]*Information provided by dr. Ingmar Stade (BIO) based on simulations*
Parameter for cell reformation	not applicable	not yet available; TBD	[d]*Information will be provided by TUG during the project*
Occurrence of perforation in animal trial	not applicable	yes/no; TBD	[d]*Information to be provided by dr. Arndt (BIO) as result of prospective animal trials*

Table 4: Ranges of the model-derived model outputs of interest for heart failure patients, both before and after PAPS implantation. The ranges are either given as mean ± standard deviation or as median (interquartile range).

Future work

In the design phase of SIMCor we have decided to select an iterative approach (*Figure 3*) for virtual cohort development and validation. The advantage is that we will generate cohorts that can iteratively be improved when new data becomes available (amongst others new patients that are outside the input space, new data extracted from clinical scans and/or functional measurements in WP5 and WP6), or when new insights acquired during SIMCor will further improve our physiological models. Note that patient-specific simulations that will be done during SIMCor will increase the accuracy of all model-derived outputs and their ranges. We believe that these patient-specific simulations are not only needed to validate our virtual cohort generator but that they are also indispensable because a lot of different WSS-based metrics are used that are not always clearly defined. It is often unclear what metric was used exactly and at which spatial position it was determined.

Our iterative approach will thus guarantee that our virtual cohorts always comply with the state-of-the-art. The virtual cohort generator will therefore be designed in a way that allows for iterative improvement. Note that the output ranges in this document might thus also be updated in later phases of the project.

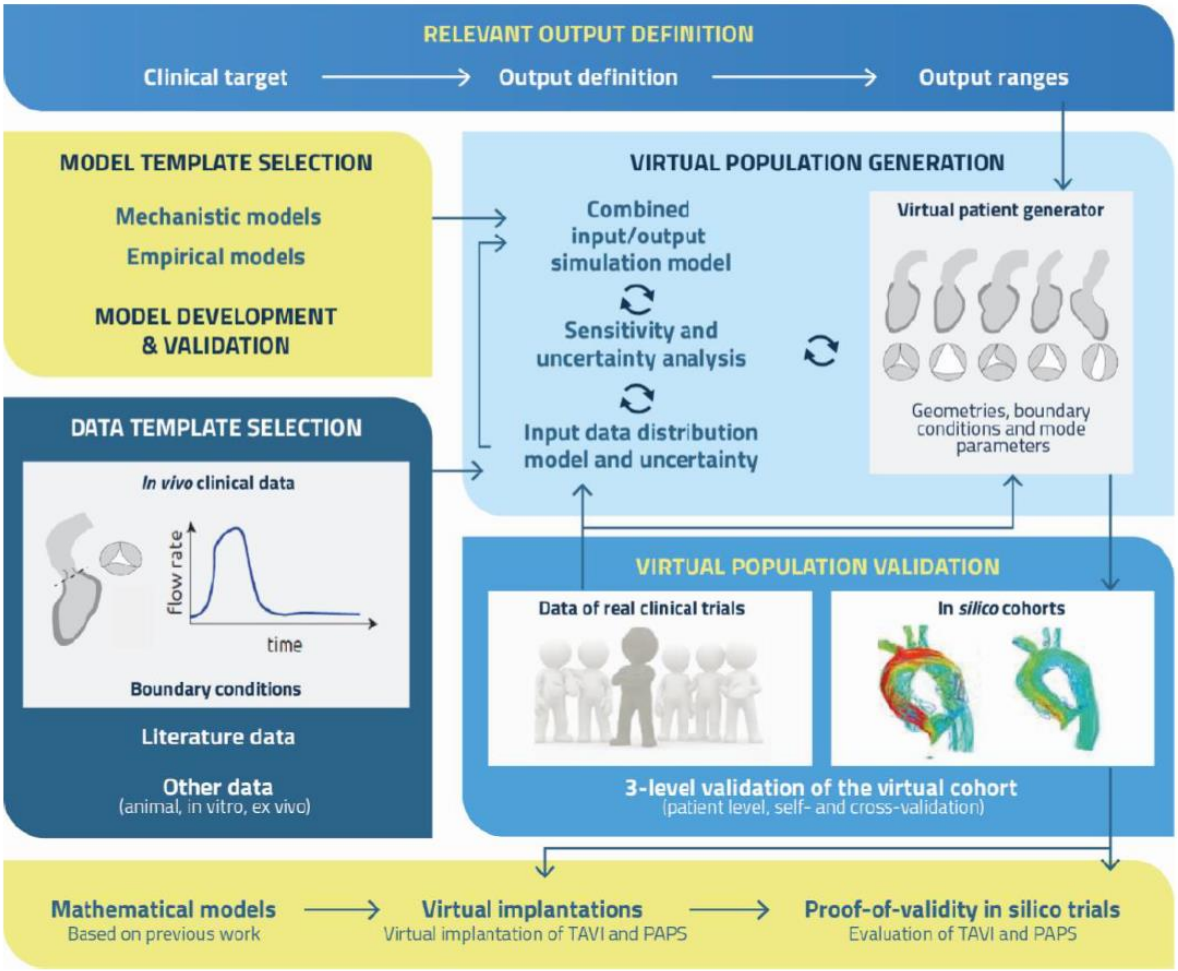

Figure 3: SIMCor methodology of virtual cohort generation and validation.